

EQUILIBRIUM MOLECULAR STRUCTURE OF 3-CYANO-4-AMINO-1,2,5-OXADIAZOLE- 2-OXIDE IN THE GAS PHASE*

N. V. Lobanov^{1,2**}, A. N. Rykov¹,
A. V. Stepanova¹, A. A. Larin³, L. L. Fershtat³,
and I. F. Shishkov¹

The molecular structure of 3-cyano-4-amino-1,2,5-oxadiazole-2-oxide (3-cyano-4-aminofuroxan, CAFO) in the gas phase is studied for the first time by gas-phase electron diffraction (GED) and quantum chemical calculations, and the equilibrium parameters of this molecule are determined. The data obtained are compared with those of related compounds analyzed by GED and single crystal X-ray diffraction. It is shown that the best agreement with the experiment is obtained at the B3LYP/aug-cc-pVTZ level of theory. The information on the molecular structure of free CAFO will be useful for the structural studies of compounds containing furoxan moieties.

DOI: 10.1134/S0022476624080110

Keywords: equilibrium molecular structure, 3-cyano-4-aminofuroxan, oxadiazoles, furoxans, gas-phase electron diffraction, quantum chemical calculations.

INTRODUCTION

1,2,5-Oxadiazoles belong to a practically important class of heterocyclic compounds being of interest for producing new pharmacologically active substances or energy-intensive systems. 1,2,5-Oxadiazole derivatives have a high enthalpy of formation and can be a promising basis for high-energy materials [1-3]. As regards their molecular structure, amino-1,2,5-oxadiazoles are suitable precursors in the synthesis of nitro derivatives: practice shows that incorporation of a nitro group into the oxadiazole ring increases the density and detonation parameters of the resulting structures [4]. However, it is worth noting that, depending on various substituents bonded to the 1,2,5-oxadiazole moiety, the properties of the compounds can vary. Hence, disadvantages of some substances of this series in terms of their practical application are low thermal and chemical stability and high sensitivity to mechanical stresses [5].

3-Cyano-4-amino-1,2,5-oxadiazole-2-oxide (3-cyano-4-aminofuroxan, CAFO) is one of the key precursors of the furoxan series, which is widely used for the synthesis of various high-energy materials [6-10]. Despite recent significant progress in this area [11-14], information on the thermal and energy properties of some functionally substituted furoxans

¹Moscow State University, Moscow, Russia. ²Joint Institute for High Temperatures, Russian Academy of Sciences, Moscow, Russia; **lnw94@yandex.ru. ³Zelinsky Institute of Organic Chemistry, Russian Academy of Sciences, Moscow, Russia. Original article submitted April 11, 2024; revised April 19, 2024; accepted April 19, 2024.

* Supplementary materials for this article are available at doi 10.1134/S0022476624080110 and are accessible for authorized users.

remains scarce. At the same time, as complete data as possible on the diverse set of compounds under consideration and profound structure–property relationships are significant for a targeted and diversity-oriented synthesis of novel promising energy materials.

The work aims to determine the equilibrium structure of the CAFO molecule in the absence of intermolecular interactions in the gas phase by gas-phase electron diffraction (GED) and quantum chemical calculations and to compare the GED and single crystal X-ray diffraction (XRD) results with the reported ones on the molecular structures of a number of related compounds.

EXPERIMENTAL

GED. A CAFO sample used in this work was obtained at the Laboratory of Nitrogen-Containing Compounds, Institute of Organic Chemistry, Russian Academy of Sciences (the sample purity is at least 99%). The spectral and analytical data (supplementary materials, Fig. S1, S2, S3) are fully consistent with the structure of the target compound. ^1H NMR spectrum (DMSO- d_6 , 300 MHz), δ_{H} (ppm): 7.13 (s, 2H). ^{13}C NMR spectrum (DMSO- d_6 , 75.5 MHz), δ_{C} (ppm): 93.5, 107.1, 156.2. IR spectrum (FTIR), cm^{-1} : 3387, 3313, 2240, 1691, 1591, 1568, 1487, 1164, 1000, 854. Elemental analysis, found (%): C 28.51, H 1.65, N 44.28, $\text{C}_3\text{H}_2\text{N}_4\text{O}_2$; calculated (%): C 28.58, H 1.60, N 44.44. The GED experiment was carried out on an EG-100M apparatus (Faculty of Chemistry, Moscow State University) for two nozzle-to-plate distances: short (SD) and long (LD). For each distance, a GED pattern was recorded on three plates (an accelerating voltage of 60 kV was used to generate the electron beam with a wavelength λ of about 0.05 Å), and the electron wavelengths were refined by the experiment with the standard substance (CCl_4) conducted at room temperature (25 °C). Full information on the experiment is given in Table 1. All GED patterns were recorded on MACO EM-FILM EMS films and scanned on an Epson Perfection 4990 scanner. The scanner was calibrated using a Standard IT8 Target (ISO 12641-1 compliant 1997) (Fuji transparency Individually measured Target) on a gray scale. The GED patterns were converted into the intensity curves using UNEX [15] (Fig. 1).

Quantum chemical calculations. The quantum chemical calculations were performed using the Gaussian09 software [16] by the DFT method with the B3LYP density functional [17, 18] and perturbation theory (MP2) [19] with 6-31G(d,p) [20], cc-pVTZ [21], and aug-cc-pVTZ [22] basis sets, and also by the CCSD(T) method [23] with the 6-31G(d,p) basis set [20]. To determine the CAFO parameters, the geometry was fully optimized. Atomic numbering in the studied molecule is given in Fig. 2 and the radial distribution curve is shown in Fig. 3.

The optimized orthogonal coordinates of CAFO determined at the CCSD(T)/6-31G(d,p), B3LYP/6-31G(d,p), and MP2/cc-pVTZ levels of theory are reported in Supplementary Materials (Tables S4, S5, and S6).

To obtain the equilibrium molecular parameters from the GED experiment, which are directly compared with those from the quantum chemical calculations, cubic force fields at the B3LYP/6-31G(d,p) level of theory were used to determine the perpendicular vibration corrections to internuclear distances [24], as well as vibrational amplitudes (supplementary

TABLE 1. Conditions of the GED Experiment

Parameter	Short distance (SD)	Long distance (LD)
Nozzle–plate distance D , Mm	193.9	362.3
Accelerating voltage U , kV	60	60
Electron beam current I , μA	3.0	2.8
Wavelength λ , Å	0.04914	0.04879
Nozzle temperature T , K	375	373
Residual pressure P , Hg mm	3.0×10^{-5}	4.0×10^{-5}
Exposition t , s	60, 50, 45	35, 35, 25
Range of scattering intensities $^{\#1} s$, Å $^{-1}$	6.6-31.2	3.4-20.0

$^{\#1} s = 4\pi\lambda^{-1}\sin(\theta/2)$, where θ is the scattering angle; λ is he electron wavelength; a step on the scale s is 0.2 Å $^{-1}$.

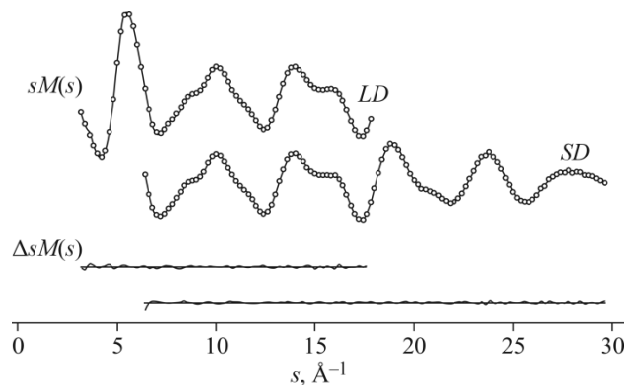


Fig. 1. Molecular intensity curves $sM(s)$ for the long (LD) and short (SD) nozzle-plate distances for the CAFO molecule. The experimental values are depicted by circles and the theoretical $sM(s)$ are shown by the solid line. The $\Delta sM(s) = sM(s)_{\text{exp}} - sM(s)_{\text{theor}}$ differences are also shown.

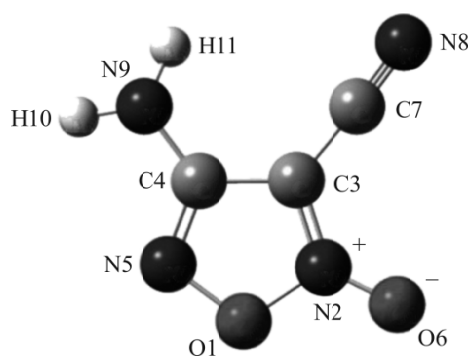


Fig. 2. Atomic numbering in the molecule of 3-cyano-4-aminofuroxan (CAFO).

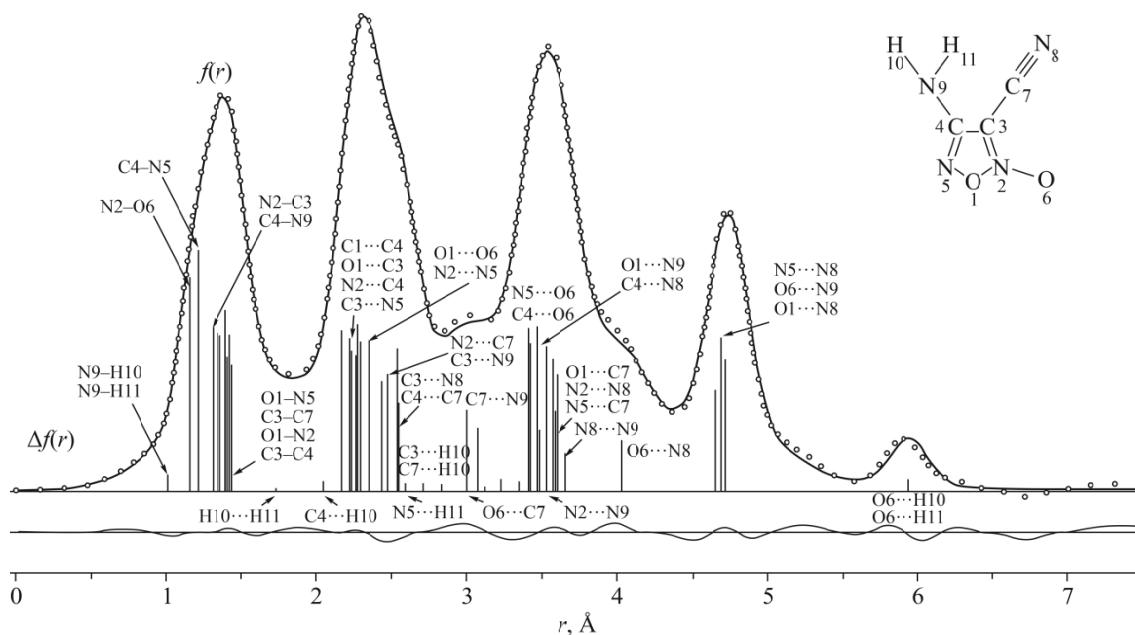


Fig. 3. Experimental (circles) and theoretical (solid line) radial distribution curves $f(r)$ for CAFO and their differences $\Delta f(r) = f(r)_{\text{exp}} - f(r)_{\text{theor}}$.

materials, Table S7) derived from the VibModule program [25]. The NBO analysis of CAFO was carried out based on the B3LYP/aug-cc-pVTZ method using the NBO 7.0 program [26].

RESULTS AND DISCUSSION

The validity that can be achieved by quantum chemical calculations depends on the method and the completeness of the basis function set [27].

Table 2 lists the optimized equilibrium parameters for CAFO, which are compared with those obtained from the theoretical calculations of 3,4-dicyanofuroxan (DCFO).

TABLE 2. Comparison of the Structural Parameters of CAFO with the Theoretical Calculations for DCFO (bond lengths in Å, bond angles in degrees, R_f in percents)

Parameter	GED ^{#1} (CAFO)	B3LYP				
		/cc-pVTZ (DCFO) [26]	/6-31G(<i>d,p</i>) (CAFO)	/cc-pVTZ (CAFO)	/aug-cc-pVTZ (CAFO)	
$r_e(\text{O1-N2})$	1.415(12)	1.472	1.425	1.420	1.419	
$r_e(\text{N2=C3})$	1.340(4)	1.340	1.347	1.342	1.341	
$r_e(\text{C3-C4})$	1.430(6)	1.425	1.432	1.428	1.428	
$r_e(\text{C4=N5})$	1.306(2)	1.306	1.314	1.306	1.306	
$r_e(\text{O1-N5})$	1.390(3)	1.346	1.392	1.389	1.390	
$r_e(\text{N2-O6})$	1.207(3)	1.195	1.213	1.205	1.206	
$r_e(\text{C3-C7})$	1.403(2)	1.405	1.407	1.403	1.403	
$r_e(\text{C7=N8})$	1.153(3)	1.152	1.164	1.154	1.153	
$r_e(\text{N9-H10})$	1.002(12)	–	1.010	1.006	1.006	
$\angle(\text{O1-N2-C3})$	106.7(3)	105.2	106.6	106.6	106.7	
$\angle(\text{N2-C3-C4})$	106.9(3)	106.9	106.8	106.9	106.9	
$\angle(\text{C3-C4-N5})$	110.9(2)	111.4	110.0	110.9	110.9	
$\angle(\text{O1-N5-C4})$	106.7(2)	107.6	106.5	106.7	106.7	
$\angle(\text{N2-O1-N5})$	108.8(3)	108.9	109.0	108.9	108.9	
$\angle(\text{O1-N2-O6})$	119.2(3)	119.0	119.2	119.2	119.2	
$\angle(\text{C3-N2-O6})$	134.0(4)	135.8	134.2	134.2	134.1	
$\angle(\text{N2-C3-C7})$	123.4(5)	122.2	123.2	123.3	123.4	
$\angle(\text{C4-C3-C7})$	129.8(2)	130.9	130.0	129.8	129.7	
$\angle(\text{C3-C7-N8})$	176.4(6)	179.0	176.5	176.3	176.2	
$\angle(\text{C4-N9-H10})$	117.5(8)	–	117.0	117.2	117.7	
$\angle(\text{H10-N9-H11})$	115.5(3)	–	115.0	115.1	115.5	
$D(\text{O1-N2-C3-C4})$	–0.3(2) ^{#2}	0.0	–0.2	–0.2	–0.1	
$D(\text{N2-O1-N5-C4})$	–0.7(2) ^{#2}	0.0	–0.9	–0.8	–0.7	
$D(\text{C3-C4-N5-O1})$	0.5(1) ^{#2}	0.0	0.7	0.7	0.6	
$D(\text{C4-N9-H10-H11})$	142.7(5) ^{#2}	–	140.3	141.5	143.8	
R_f LD	3.1					
R_f SD	5.5					
R_f total	4.3					
Parameter	MP2				CCSD(T)	
	/cc-pVTZ (DCFO) [26]	/6-31G(<i>d,p</i>) (CAFO)	/cc-pVTZ (CAFO)	/aug-cc-pVTZ (CAFO)	/6-31G(<i>d,p</i>) (DCFO) [26]	/6-31G(<i>d,p</i>) (CAFO)
1	2	3	4	5	6	7
$r_e(\text{O1-N2})$	1.552 ^{#3}	1.459	1.435	1.435	1.455	1.423
$r_e(\text{N2=C3})$	1.354	1.354	1.349	1.348	1.344	1.338
$r_e(\text{C3-C4})$	1.403	1.415	1.411	1.411	1.422	1.430
$r_e(\text{C4=N5})$	1.337	1.326	1.319	1.320	1.314	1.310
$r_e(\text{O1-N5})$	1.314	1.364	1.356	1.358	1.361	1.387
$r_e(\text{N2-O6})$	1.194	1.225	1.214	1.217	1.202	1.215
$r_e(\text{C3-C7})$	1.408	1.412	1.406	1.406	1.416	1.421

TABLE 2. (Cont.)

1	2	3	4	5	6	7
$r_c(\text{C7}\equiv\text{N8})$	1.174	1.185	1.174	1.174	1.164	1.167
$r_c(\text{N9-H10})$	–	1.010	1.008	1.009	–	1.009
$\angle(\text{O1-N2-C3})$	102.1	104.9	105.3	105.4	105.8	106.8
$\angle(\text{N2-C3-C4})$	109.0	108.0	107.7	107.7	–	106.8
$\angle(\text{C3-C4-N5})$	111.6	110.6	110.2	110.2	–	110.9
$\angle(\text{O1-N5-C4})$	108.2	107.4	107.5	107.4	–	106.5
$\angle(\text{N2-O1-N5})$	109.0	109.1	109.3	109.3	109.0	108.9
$\angle(\text{O1-N2-O6})$	119.9	119.4	119.4	119.4	118.9	118.9
$\angle(\text{C3-N2-O6})$	138.0	135.7	135.3	135.3	–	134.4
$\angle(\text{N2-C3-C7})$	120.3	121.2	121.9	122.0	121.9	122.4
$\angle(\text{C4-C3-C7})$	130.6	130.8	130.4	130.3	–	130.8
$\angle(\text{C3-C7-N8})$	179.7	177.4	177.0	176.7	179.0	176.9
$\angle(\text{C4-N9-H10})$	–	114.1	114.2	114.8	–	114.6
$\angle(\text{H10-N9-H11})$	–	111.8	112.2	112.8	–	112.4
$D(\text{O1-N2-C3-C4})$	0.0	–1.5	–0.4	–0.4	0.0	–0.7
$D(\text{N2-O1-N5-C4})$	0.0	–0.9	–0.9	–0.8	–	–0.7
$D(\text{C3-C4-N5-O1})$	0.0	0.0	0.6	0.6	–	0.3
$D(\text{C4-N9-H10-H11})$	–	128.5	129.8	131.9	–	130.6

#1 Errors were determined as 3σ -LSM; i.e., they are equal to the triple standard deviation by LSM.

#2 Initial approximation was determined at the B3LYP/6-31G(*d,p*) level of theory.

#3 The authors pay attention to the overestimated value in the calculation of the MP2/cc-pVTZ O1-N2 bond to 1.552 Å compared to 1.459(4) Å and 1.415(12) Å for DCFO and CAFO, respectively. Apparently, this calculation method gives an overestimated result for these objects.

Table 2 demonstrates some differences between our calculated geometric parameters for the two compounds under consideration. It can be assumed that amino group substitution for one of the cyano groups in DCFO markedly affects the molecular electron density distribution, and hence, the bond lengths and angles. For CAFO in the MP2/cc-pVTZ approximation, the calculated lengths of some bonds between heteroatoms in the molecular ring increased compared to the respective B3LYP/cc-pVTZ data, except for the $r_c(\text{O1-N5})$ bond whose length decreased. The results of the analogous CCSD(T)/6-31G(*d,p*) calculation show a similar trend, although to a slightly lesser extent [28].

Table 2 evidences that the CCSD(T)/6-31G(*d,p*) level of theory is in good agreement with the experimental data and generally reproduces the GED results within the experimental error range, yet the $r_c(\text{C3-C7})$ bond length is overestimated by approximately 0.02 Å. The MP2 results are beyond the experimental error; the bond lengths are overestimated on average by 0.01 Å, and for $r_c(\text{O1-N5})$ the final MP2/aug-cc-pVTZ result is underestimated by 0.03 Å. The B3LYP functional provides the best agreement (especially, the aug-cc-pVTZ basis set), almost always falling into the experimental error range. It can be noted that the results at the B3LYP/6-31G(*d,p*) level of theory, if they do not coincide with the experimental molecular parameters, almost always exceed them approximately by the same value of 0.003-0.008 Å for bond lengths and by 0.2-0.7° for bond angles (Table 2). Moreover, this method gives good values within the GED error range when determining the bond angles.

Having analyzed the considered methods, it can be assumed that the values closest to the experiment can be obtained at the B3LYP/aug-cc-pVTZ level of theory; and slightly worse, in the B3LYP/6-31G(*d,p*) approximation.

The work also compares the CAFO structural parameters with the geometry of structurally similar compounds (DCFO, 3-methyl-4-nitrofuroxan, and 4-methyl-3-nitrofuroxan), which were determined by GED in [29, 30]. The results are presented in Table 3.

The largest differences are observed for $r_c(\text{O1-N2})$ (about 0.04 Å) and $r_c(\text{O1-N5})$ (approximately 0.03 Å) bonds. The other values for the CAFO-DCFO pair differ by no more than 0.01 Å. This may be due to the presence of an additional cyano group—an electron density acceptor that pulls part of the electron cloud onto itself. This distorts the oxadiazole ring,

TABLE 3. Comparison of the Structural Parameters of 3-Cyano-4-Aminofuroxan, Dicyanofuroxan, 3-Methyl-4-Nitrofuroxan, and 4-Methyl-3-Nitrofuroxan

Parameter ^{#1}	CAFO GED ^b	DCFO GED [29]	3-methyl-4-nitrofuroxan GED [30]	4-methyl-3-nitrofuroxan GED [30]
$r_c(\text{O1-N2})$	1.415(12)	1.459(5)	1.462(9)	1.382(6)
$r_c(\text{N2=C3})$	1.340(3)	1.331(3)	1.333(9)	1.307(6)
$r_c(\text{C3-C4})$	1.430(6)	1.419(2)	1.414(9)	1.422(6)
$r_c(\text{C4=N5})$	1.306(2)	1.299(3)	1.304(9)	1.340(6)
$r_c(\text{O1-N5})$	1.390(3)	1.367(5)	1.354(9)	1.429(6)
$r_c(\text{N2-O6})$	1.207(3)	1.199(4)	1.215(9)	1.205(6)
$r_c(\text{C3-C7})$	1.403(2)	1.399(2)	1.488(9)	1.488(6)
$\angle(\text{O1-N2-C3})$	106.7(3)	105.0(4)	107.2(5)	107.5(3)
$\angle(\text{N2-C3-C4})$	106.9(3)	107.1(6)	104.6(5)	109.2(3)
$\angle(\text{C3-C4-N5})$	110.9(2)	111.7(3)	113.9(5)	109.2(3)
$\angle(\text{O1-N5-C4})$	106.7(2)	107.9(3)	106.1(10)	104.7(4)
$\angle(\text{N2-O1-N5})$	108.8(3)	108.8(3)	108.1(10)	109.4(5)
$\angle(\text{O1-N2-O6})$	119.2(3)	119.3(6)	118.1(6)	118.6(3)
$\angle(\text{N2-C3-C7})$	123.4(5)	122.6(3)	121.2(5)	121.1(3)

^{#1} The bond lengths are in Å, the bond angles are in degrees.

which is manifested in a change in bond lengths, although the considered angles formed by atoms of the compounds often coincide or differ by no more than 1° (except for $\angle(\text{O1-N2-C3})$).

The NBO analysis based on the B3LYP/aug-cc-pVTZ method showed that amino group substitution for the cyano group disturbs the general conjugation of the π electron system. Consequently, the Wiberg indices decrease for all bonds approximately by 4-7%, except the index of the bond between the cyano carbon atom and the carbon atom in the oxadiazole ring, which increased by 5% (Fig. 4). It is also clear that a greater effective charge is concentrated on heteroatoms.

In addition, we compared the $\text{C}\equiv\text{N}$ bond lengths in the CAFO and DCFO molecules and in a series of cyanopyridines, for which the structural data were obtained by two experimental methods: GED and single crystal XRD (Table 4).

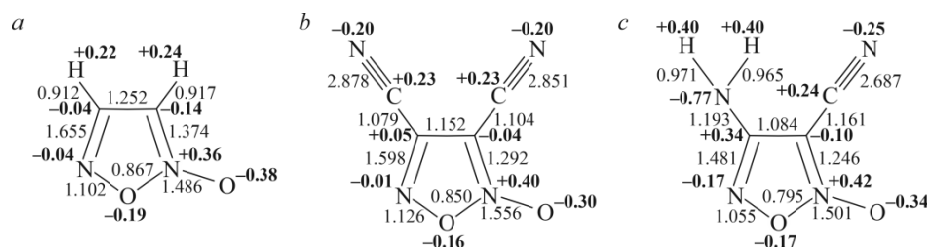


Fig. 4. Wiberg indices and the effective atomic charges in the molecules of furoxan (a), DCFO (b), and CAFO (c).

TABLE 4. Comparison of the Bond Lengths (Å) $\text{C}\equiv\text{N}$ in the CAFO-DCFO-2-Cyanopyridine-3-Cyanopyridine-4-Cyanopyridine Series

CAFO GED	DCFO (GED) [29]		2-cyanopyridine [31]		3-cyanopyridine [32]		4-cyanopyridine [33]	
$r_c(\text{C7}\equiv\text{N8})$	$r_c(\text{C7}\equiv\text{N8})$	$r_c(\text{C9}\equiv\text{N10})$	GED	XRD	GED	XRD	GED	XRD
1.153(3)	1.164(3)	1.162(3)	1.158(5)	1.1452(8)	1.157(2)	1.1499(12)	1.159(3)	1.1370(8)

It can be seen that the experimental C≡N bond length for CAFO slightly differs from that in the other molecules by approximately 1-1.5%, although this value falls within the acceptable range observed in the series of compounds under consideration.

CONCLUSIONS

The molecular structure of CAFO in the gas phase was studied for the first time by GED and quantum chemical calculations, and its equilibrium parameters were determined. The data obtained were compared with the analogous data for the related compounds analyzed by GED and single crystal XRD. It was demonstrated that the best agreement with the experiment was obtained at the B3LYP/aug-cc-pVTZ level of theory.

It was shown that the presence of only one cyano group as a substituent compared to DCFO distorted the geometry of the studied molecule: the $r_c(\text{O1-N2})$ bond shortens by 0.045 Å and $r(\text{O1-N5})$ elongates by 0.02 Å, the O1-N2-C3 bond angle increases by 1.7°.

The NBO analysis at the B3LYP/aug-cc-pVTZ level of theory shows that the cyano group is an electron density acceptor and, therefore, concentrates part of the electron cloud on itself. Unlike DCFO, CAFO is to a lesser extent a coupled π electron system, hence, a larger effective charge is concentrated on more electronegative atoms (Fig. 4).

Furthermore, differences were found between the CAFO molecular structure and the structures of related 3-methyl-4-nitrofuloxan and 4-methyl-3-nitrofuloxan: $r_c(\text{O1-N2})$ and $r_c(\text{O1-N5})$ bond lengths differ on average by ± 0.04 Å, suggesting a strong effect of nitro groups on the five-membered ring geometry. The comparison of bond lengths and bond angles generally reveals the discrepancy: the CAFO parameters differ on average by 0.03 Å of the respective pair of 3-methyl-4-nitrofuloxan and 4-methyl-3-nitrofuloxan parameters.

The information obtained on the molecular structure of free CAFO will be useful for the structural studies of compounds containing fuloxan moieties.

FUNDING

N. V. Lobanov, A. N. Rykov, A. V. Stepanova, and I. F. Shishkov are grateful for the support of the work within the State Task “The molecular structure and supramolecular organization of individual substances, hybrid and functional materials” (CITIS number: 121031300090-2); N. V. Lobanov is grateful and also notes that the work was supported by the State Task for the Joint Institute for High Temperatures, Russian Academy of Sciences, 2024 (No. 075-00270-24-00, 27.12.2023).

CONFLICT OF INTERESTS

The authors of this work declare that they have no conflicts of interest.

REFERENCES

1. L. L. Fershtat and N. N. Makhova. 1,2,5-Oxadiazole-based high-energy-density materials: Synthesis and performance. *ChemPlusChem*, **2020**, 85(1), 13-42. <https://doi.org/10.1002/cplu.201900542>
2. A. A. Larin and L. L. Fershtat. Energetic heterocyclic N-oxides: Synthesis and performance. *Mendeleev Commun.*, **2022**, 32(6), 703-713. <https://doi.org/10.1016/j.mencom.2022.11.001>
3. N. N. Makhova and A. S. Kulikov. Advances in the chemistry of monocyclic amino- and nitrofuloxans. *Russ. Chem. Rev.*, **2013**, 82(11), 1007-1033. <https://doi.org/10.1070/rc2013v082n11abeh004369>

4. A. A. Larin, A. V. Shaferov, M. A. Epishina, I. N. Melnikov, N. V. Muravyev, I. V. Ananyev, L. L. Fershtat, and N. N. Makhova. Pushing the energy-sensitivity balance with high-performance bifuroxans. *ACS Appl. Energy Mater.*, **2020**, 3(8), 7764-7771. <https://doi.org/10.1021/acsaem.0c01162>
5. N. V. Muravyev, D. B. Meerov, K. A. Monogarov, I. N. Melnikov, E. K. Kosareva, L. L. Fershtat, A. B. Sheremetev, I. L. Dalinger, I. V. Fomenkov, and A. N. Pivkina. Sensitivity of energetic materials: Evidence of thermodynamic factor on a large array of CHNOFCl compounds. *Chem. Eng. J.*, **2021**, 421, 129804. <https://doi.org/10.1016/j.cej.2021.129804>
6. E. C. Johnson, J. J. Sabatini, D. E. Chavez, L. A. Wells, J. E. Banning, R. C. Sausa, E. F. C. Byrd, and J. A. Orlicki. Bis(nitroxymethylisoxazolyl) furoxan: A promising standalone melt-castable explosive. *ChemPlusChem*, **2020**, 85(1), 237-239. <https://doi.org/10.1002/cplu.201900710>
7. L. Zhai, F. Bi, Y. Luo, N. Wang, J. Zhang, and B. Wang. New strategy for enhancing energetic properties by regulating trifuroxan configuration: 3,4-Bis(3-nitrofuroxan-4-yl)furoxan. *Sci. Rep.*, **2019**, 9(1), 4321. <https://doi.org/10.1038/s41598-019-39723-z>
8. A. A. Larin, N. V. Muravyev, A. N. Pivkina, K. Y. Suponitsky, I. V. Ananyev, D. V. Khakimov, L. L. Fershtat, and N. N. Makhova. Assembly of tetrazolylfuroxan organic salts: multipurpose green energetic materials with high enthalpies of formation and excellent detonation performance. *Chem. - Eur. J.*, **2019**, 25(16), 4225-4233. <https://doi.org/10.1002/chem.201806378>
9. A. A. Larin, A. V. Shaferov, K. A. Monogarov, D. B. Meerov, A. N. Pivkina, and L. L. Fershtat. Novel energetic oxadiazole assemblies. *Mendeleev Commun.*, **2022**, 32(1), 111-113. <https://doi.org/10.1016/j.mencom.2022.01.036>
10. A. A. Larin, D. D. Degtyarev, I. V. Ananyev, A. N. Pivkina, and L. L. Fershtat. Linear furoxan assemblies incorporating nitrobifuroxan scaffold: En route to new high-performance energetic materials. *Chem. Eng. J.*, **2023**, 470, 144144. <https://doi.org/10.1016/j.cej.2023.144144>
11. I. D. Deltsov, I. V. Ananyev, D. B. Meerov, and L. L. Fershtat. Expanding the limits of organic energetic materials: High-performance alliance of 1,3,4-thiadiazole and furazan scaffolds. *J. Org. Chem.*, **2024**, 89(1), 174-182. <https://doi.org/10.1021/acs.joc.3c01858>
12. A. V. Shaferov, S. T. Arakelov, F. E. Teslenko, A. N. Pivkina, N. V. Muravyev, and L. L. Fershtat. First example of 1,2,5-oxadiazole-based hypergolic ionic liquids: A new class of potential energetic fuels. *Chem. - Eur. J.*, **2023**, 29(44). <https://doi.org/10.1002/chem.202300948>
13. M. A. Epishina, A. S. Kulikov, I. V. Ananyev, A. A. Anisimov, K. A. Monogarov, and L. L. Fershtat. Impact of regiochemistry in energetic materials science: A case of (nitratomethyl-1,2,3-triazolyl)furoxans. *Dalton Trans.*, **2023**, 52(22), 7673-7683. <https://doi.org/10.1039/d3dt00917c>
14. A. A. Larin, A. N. Pivkina, I. V. Ananyev, D. V. Khakimov, and L. L. Fershtat. Novel family of nitrogen-rich energetic (1,2,4-triazolyl) furoxan salts with balanced performance. *Front. Chem.*, **2022**, 10. <https://doi.org/10.3389/fchem.2022.1012605>
15. Y. V. Vishnevskiy. UNEX 1.6-1075-gd85e256d, <http://unexprog.org>.
16. Gaussian 09, Revision A.02. M. J. Frisch, G. W. Trucks, H. B. Schlegel, G. E. Scuseria, M. A. Robb, J. R. Cheeseman, G. Scalmani, V. Barone, G. A. Petersson, H. Nakatsuji, X. Li, M. Caricato, A. Marenich, J. Bloino, B. G. Janesko, R. Gomperts, B. Mennucci, H. P. Hratchian, J. V. Ortiz, A. F. Izmaylov, J. L. Sonnenberg, D. Williams-Young, F. Ding, F. Lipparini, F. Egidi, J. Goings, B. Peng, A. Petrone, T. Henderson, D. Ranasinghe, V. G. Zakrzewski, J. Gao, N. Rega, G. Zheng, W. Liang, M. Hada, M. Ehara, K. Toyota, R. Fukuda, J. Hasegawa, M. Ishida, T. Nakajima, Y. Honda, O. Kitao, H. Nakai, T. Vreven, K. Throssell, J. A. Montgomery Jr., J. E. Peralta, F. Ogliaro, M. Bearpark, J. J. Heyd, E. Brothers, K. N. Kudin, V. N. Staroverov, T. Keith, R. Kobayashi, J. Normand, K. Raghavachari, A. Rendell, J. C. Burant, S. S. Iyengar, J. Tomasi, M. Cossi, J. M. Millam, M. Klene, C. Adamo, R. Cammi, J. W. Ochterski, R. L. Martin, K. Morokuma, O. Farkas, J. B. Foresman, and D. J. Fox. Wallingford, CT, USA: Gaussian, **2016**.
17. A. D. Becke. Density-functional exchange-energy approximation with correct asymptotic behavior. *Phys. Rev. A*, **1988**, 38(6), 3098-3100. <https://doi.org/10.1103/physreva.38.3098>

18. C. Lee, W. Yang, and R. G. Parr. Development of the Colle-Salvetti correlation-energy formula into a functional of the electron density. *Phys. Rev. B*, **1988**, 37(2), 785-789. <https://doi.org/10.1103/physrevb.37.785>
19. C. Møller and M. S. Plesset. Note on an approximation treatment for many-electron systems. *Phys. Rev.*, **1934**, 46(7), 618-622. <https://doi.org/10.1103/physrev.46.618>
20. G. A. Petersson, A. Bennett, T. G. Tensfeldt, M. A. Al-Laham, W. A. Shirley, and J. Mantzaris. A complete basis set model chemistry. I. The total energies of closed-shell atoms and hydrides of the first-row elements. *J. Chem. Phys.*, **1988**, 89(4), 2193-2218. <https://doi.org/10.1063/1.455064>
21. T. H. Dunning. Gaussian basis sets for use in correlated molecular calculations. I. The atoms boron through neon and hydrogen. *J. Chem. Phys.*, **1989**, 90(2), 1007-1023. <https://doi.org/10.1063/1.456153>
22. R. A. Kendall, T. H. Dunning, and R. J. Harrison. Electron affinities of the first-row atoms revisited. Systematic basis sets and wave functions. *J. Chem. Phys.*, **1992**, 96(9), 6796-6806. <https://doi.org/10.1063/1.462569>
23. G. E. Scuseria and T. J. Lee. Comparison of coupled-cluster methods which include the effects of connected triple excitations. *J. Chem. Phys.*, **1990**, 93(8), 5851-5855. <https://doi.org/10.1063/1.459684>
24. V. A. Sipachev. Anharmonic corrections to structural experiment data. *Struct. Chem.*, **2000**, 11, 167-172. <https://doi.org/10.1023/a:1009217826943>
25. Y. V. Vishnevskiy and Y. A. Zhabanov. New implementation of the first-order perturbation theory for calculation of interatomic vibrational amplitudes and corrections in gas electron diffraction. *J. Phys. Conf. Ser.*, **2015**, 633, 012076. <https://doi.org/10.1088/1742-6596/633/1/012076>
26. E. D. Glendening, C. R. Landis, and F. Weinhold. NBO 7.0: New vistas in localized and delocalized chemical bonding theory. *J. Comput. Chem.*, **2019**, 40(25), 2234-2241. <https://doi.org/10.1002/jcc.25873>
27. T. Helgaker, P. Jørgensen, and J. Olsen. *Molecular Electronic Structure Theory*. Chichester, England: Wiley, **2000**.
28. I. N. Kolesnikova, N. V. Lobanov, V. N. Lobanov, and I. F. Shishkov. Quantum chemical research of the molecular structure of 3,4-dicyanofuroxan. *Fine Chem. Technol.*, **2023**, 18(2), 98-108. <https://doi.org/10.32362/2410-6593-2023-18-2-98-108>
29. I. N. Kolesnikova, S. V. Kolesnikov, N. V. Lobanov, P. Yu. Sharanov, A. A. Larin, F. E. Teslenko, L. L. Fershtat, and I. F. Shishkov. Molecular structure of 3,4-dicyanofuroxan studied by gas electron diffraction. Application of DFT theory and coupled cluster computations. *Chem. Phys. Lett.*, **2023**, 829, 140770. <https://doi.org/10.1016/j.cplett.2023.140770>
30. A. V. Belyakov, A. A. Oskorbin, V. A. Losev, A. N. Rykov, I. F. Shishkov, L. L. Fershtat, A. A. Larin, V. V. Kuznetsov, and N. N. Makhova. The equilibrium molecular structure of 3-methyl-4-nitro- and 4-methyl-3-nitrofuroxans by gas-phase electron diffraction and coupled cluster calculations. *J. Mol. Struct.*, **2020**, 1222, 128856. <https://doi.org/10.1016/j.molstruc.2020.128856>
31. N. Vogt, L. S. Khaikin, A. N. Rykov, O. E. Grikina, A. A. Batiukov, J. Vogt, I. V. Kochikov, and I. F. Shishkov. The equilibrium molecular structure of 2-cyanopyridine from combined analysis of gas-phase electron diffraction and microwave data and results of ab initio calculations. *Struct. Chem.*, **2019**, 30(5), 1699-1706. <https://doi.org/10.1007/s11224-019-01393-y>
32. L. S. Khaikin, N. Vogt, A. N. Rykov, O. E. Grikina, J. Vogt, I. V. Kochikov, E. S. Ageeva, and I. F. Shishkov. The equilibrium molecular structure of 3-cyanopyridine according to gas-phase electron diffraction and microwave data and the results of quantum-chemical calculations. *Mendeleev Commun.*, **2018**, 28(3), 236-238. <https://doi.org/10.1016/j.mencom.2018.05.002>
33. L. S. Khaikin, N. Vogt, A. N. Rykov, O. E. Grikina, J. Demaison, J. Vogt, I. V. Kochikov, Y. D. Shishova, E. S. Ageeva, and I. F. Shishkov. The equilibrium molecular structure of 4-cyanopyridine according to a combined analysis of gas-phase electron diffraction and microwave data and coupled-cluster computations. *Russ. J. Phys. Chem. A*, **2018**, 92(10), 1970-1974. <https://doi.org/10.1134/s0036024418100102>

Publisher's Note. Pleiades Publishing remains neutral with regard to jurisdictional claims in published maps and institutional affiliations.